Physica B: Condensed Matter 571 (2019) 64–70

Contents lists available at ScienceDirect

Physica B: Condensed Matter

journal homepage: www.elsevier.com/locate/physb

Facile fabrication and characterization of modified spray deposited cadmium sulphide thin films

S.S. Shaikh[a], Mohd Shkir[b], E.U. Masumdar[a,*]

[a] Thin Film Physics Laboratory, Department of Physics, Electronics and Photonics, Rajarshi Shahu Mahavidyalaya, Latur, 413512, Maharashtra, India
[b] Advanced Functional Materials & Optoelectronics Laboratory (AFMOL), Department of Physics, Faculty of Science, King Khalid University, P.O. Box 9004, Abha, 61413, Saudi Arabia

ARTICLE INFO

Keywords:
Cadmium sulphide (CdS)
Spray pyrolysis
Structural properties
Morphological properties
Optical properties
Electrical properties

ABSTRACT

Herein we have deposited the Cadmium sulphide thin films chemically on glass substrates using modified spray pyrolysis technique, at 300 °C. The thickness of the deposited film was found to be 301 nm and the film was yellow in colour. Deposited CdS films were subjected to elemental, morphological, optical, structural and electrical studies. XRD analysis revealed that film was polycrystalline in nature and grain size was found to be 15 nm with the hexagonal crystal structure. The EDX analysis confirms the presence of S & Cd elements in film in the ratio 0.77. The morphological analysis showed the needle-shaped grains with an average grain size 43 nm. Raman spectra showed that all observed peaks correspond to the longitudinal optical phonon mode. The optical direct band gap value was found to be 2.43 eV. The room temperature electrical resistivity obtained was 2.2×10^6 Ω-cm. TEP studies revealed that film exhibits n-type conductivity.

1. Introduction

Cadmium sulphide is one of the very important semiconductor compounds having applications in solar cells [1], dye-sensitized solar cells [2], solid-state gas sensors [3], nanorod superlattices [4], field effect transistor and light emitting diode [5,6] etc., due to its wide band gap, high transmittivity, low resistivity and high absorption coefficient. In solar cells, it is employed as a window layer [7]. As it has n-type semi-conductivity, it is used as a partner for p-type material in heterojunction solar cell [8]. The quantum confinement of semiconductor materials like CdS is very useful in tailoring their electronic and optical properties. CdS have very good structural and optical properties which are very useful from the point of efficient solar energy conversion [9,10]. Hence the investigation of these properties of CdS thin film at optimised preparative parameters is very important.

Various scientific techniques have been employed for the preparation of CdS thin films such as chemical bath deposition [11,12], spray pyrolysis [13], magnetron sputtering [14], electrodeposition [15], thermal evaporation [16], SILAR [17], vacuum evaporation [18], sol-gel [19], closed space sublimation [20], molecular beam epitaxy [21], screen printing [22] etc.

Among all these methods spray pyrolysis is a cost-effective, simple and easy technique in which pyrolytic decomposition of an ionic solution having the ions of a compound to be prepared takes place on a hot substrate [23,24]. So, spray pyrolysis technique seems to be very important and cost-effective to deposit the good quality homogeneous large area films at optimised conditions. Hence, in this paper, we have presented the elemental, morphological, optical, structural and electrical properties of the spray deposited cadmium sulphide thin films.

2. Experimental details

Cadmium sulphide thin films were prepared chemically by using modified spray pyrolysis setup, on to glass substrate. It involves the spray formation and atomisation of precursor solution which results in chemical reaction on a hot substrate. The commercial glass slides obtained from Blue Star were used as substrates which were first cleaned with labolene liquid detergent and then boiled in 1 M solution of chromic acid at 300 °C for 30 min. After cooling for 12 h followed by rinsing in double distilled water substrates were used for deposition.

To deposit the CdS thin films, 36 ml equimolar solution of cadmium chloride monohydrate A.R. ($CdCl_2.H_2O$) and Thiourea Hi-AR™/ACS (CH_4N_2S) was used. Both these solutions were of 0.025 M containing ammonia and DDW in the ratio 1:4. Before mixing with the thiourea solution, 0.5 ml triethanolamine (TEA) was added to the cadmium chloride solution. The pH of the final solution was kept at 11.5 ± 0.5. The temperature of the substrate was kept constant at 300 °C. Air was supplied at pressure 1 kg/cm^3. The solution flow rate was maintained at

* Corresponding author.
E-mail address: emasumdar@yahoo.com (E.U. Masumdar).

https://doi.org/10.1016/j.physb.2019.06.051
Received 28 May 2019; Received in revised form 20 June 2019; Accepted 22 June 2019
Available online 24 June 2019
0921-4526/

5 ml/min using a peristaltic pump. Nozzle to substrate distance was 27 cm. Under these preparative condition's deposition was carried out and after deposition film temperature was let to reach room temperature.

The thickness of the as-deposited thin films was determined using the weight difference method. The structural characterization was carried out by using X-ray diffractometer (Shimadzu LabX XRD-6000), with CuKα radiation (λ = 1.5406 Å) in the 2θ range from 20 to 80°. The morphological and elemental studies were done with the help of a 'JSM6360 LA, Japan SEM' armed with EDXS. FT-Raman spectra were recorded using 'Thermo Fisher Scientific DXR FT-Raman Spectrometer'. The optical reflectance, transmittance and absorbance studies were carried out using a 'UV–Vis–NIR spectrophotometer' (JASCO V-570) and also the related optical constants like band gap were studied and discussed. The two-probe press contact method was employed to the study of electrical conductivity. The silver paste was used for good ohmic contact in electrical and TEP studies.

3. Results and discussion

When the precursor solution was prepared and deposited, following the conditions mentioned above in experimental part, on a hot substrate, pyrolytic decomposition of the precursor solution takes place on a hot substrate which results in the formation of yellow coloured CdS thin film. The film was compact, crack-free and pinhole free. This uniform film was having good adhesion with the glass substrate.

3.1. Thickness estimation

The thickness of the as-deposited film was estimated by the weight difference technique, using the relation $t = \frac{m}{A * \rho}$, where 't' stands for the thickness of the film, m stands for the mass of film deposited on area 'A' of substrate and ρ stands for the density of material (for CdS ρ = 4.82 g/cm^3). The thickness of the as-deposited film was found to be 301 nm. The similar results with nearly the same preparative conditions were obtained by several other researchers also [25].

3.2. Structural study

Fig. 1 demonstrations the X-ray diffractogram of given thin film sample with 2θ ranging from 20 to 80° and from it is can be seen that the prominent peaks are obtained at 2θ values 24.8900, 26.5343, 28.2316, 36.7000, 43.7950, 47.8800, 51.9500 which are associated with the planes (100), (002), (101), (102), (110), (103), (112) respectively, of hexagonal crystal structure (JCPDS Card No.: 41–1049) and the corresponding calculated 'd' values are 3.57444, 3.35655, 3.15849, 2.44679, 2.06544, 1.89832, 1.75876, respectively. The (002) reflection peak has the highest intensity which shows that film fabrication is along this plane [26].

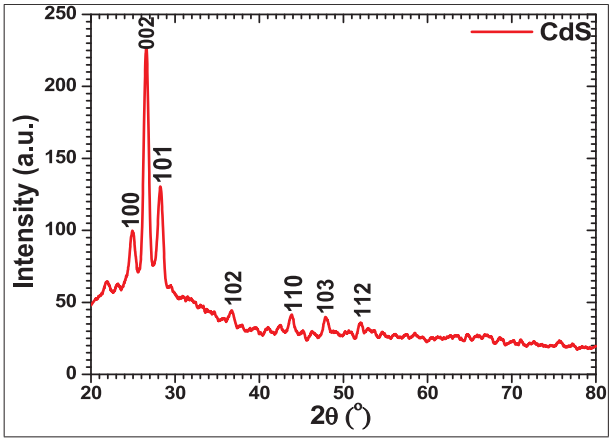

Fig. 1. X-ray diffractogram for CdS thin film prepared at 300 °C.

The crystallite size (D), lattice strain (ε), dislocation density (δ) and texture coefficient (TC) are evaluated by using the Scherrer formula and other relations as follows [27–30]:

$$D = \frac{k\lambda}{\beta \cos\theta}, \varepsilon = \frac{\beta \cos\theta}{4}, \delta = \frac{1}{D^2},$$

TC was determined along (002) by Ref. [31]:

$$TC\ (hkl\ \ ) = \frac{I\ (hkl\ \ )\ /I_0(hkl\ \ )}{N_r^{-1} \sum I\ (hkl\ \ )/I_0(hkl\ \ )}$$

where λ stands for the wavelength of X-ray, β stands for full width at half maximum (FWHM in radians) of the XRD peak, θ stands for the Bragg angle and k stands for Scherrer's constant which is '0.9' [24], $I_{(hkl)}$, and $I_{0(hkl)}$ are related to measured intensity and standard intensity from JCPDS and N is number of reflection and TC value should ~ 1. The calculated average crystallite size was 15 nm which is in good agreement with reported earlier [26,32,33]. The micro-structural parameters like lattice strain (ε), dislocation density (δ) and texture coefficient for (0 0 2) plane are found to be 2.3287 × 10^{-3}, 4.513 × 10^{-3} lines. m^{-2} and 2.840, respectively and which are in good agreement with earlier reported values [19,24]. Lattice strain is the inhomogeneous local strain in the material which gives rise to X-ray peak broadening. Dislocations are responsible for plastic deformation and determination of the dislocation density is based on the broadening of the X-ray diffraction lines. The estimated TC value is found to be higher than 1 confirming the grains orientation along [002] direction. Therefore, lattice strain, dislocation density and TC values are found to be varied accordingly.

The obtained films show a polycrystalline crystal structure with a pure hexagonal structure, which shows that the deposition has taken place ion by ion during pyrolytic decomposition. Hexagonal CdS has more stability in comparison with the cubic CdS and the hexagonal CdS is often used in heterojunction solar cell than the cubic CdS [34].

The lattice parameters 'a' and 'c' for the unit cell of the hexagonal crystal structure were evaluated using the relation [24]:

$$\frac{1}{d^2} = \frac{4}{3}\frac{h^2 + hk + k^2}{a^2} + \frac{l^2}{c^2}$$

where d is the interplanar spacing. The obtained values of lattice parameters are a = b = 4.1308 Å and c = 6.7130 Å. These evaluated values of lattice parameters are nearly equal to standard values (JCPDS Card No.: 41–1049).

3.3. Elemental and morphological analysis

The EDX spectra and SEM mapping image of as-deposited thin films were recorded as shown in Fig. 2(a and b).

The EDX spectra confirm the presence of Cadmium and Sulphur elements. The elemental analysis showed that S/Cd ratio is 0.77, the film contains excess cadmium with sulphur deficiency. The reason for sulphur deficiency within the film may be its great affinity towards oxygen, resulting in SO_2 and evaporated due to high temperature. Other than Cd and S one more peak is found in the spectra which is due to the nature of glass substrate [19,35]. Table 1 shows the as taken atomic percentage and as an observed atomic percentage of Cadmium and Sulphur elements. The obtained values are nearly the same as reported earlier [24].

The SEM photograph of the CdS thin film deposited at 300 °C is publicized in Fig. 3. Morphological properties of the prepared thin film were studied using SEM photograph. It can be seen from the image that, the thin films exhibited compact surface morphology which is free from cracks and voids. It can be also seen that the grains were of needle-shaped and were distributed over the entire surface of the film, similar type of behaviour is also observed by other researchers [24,35,36]. The effect of size of grains, shapes, doping and thickness of films are very

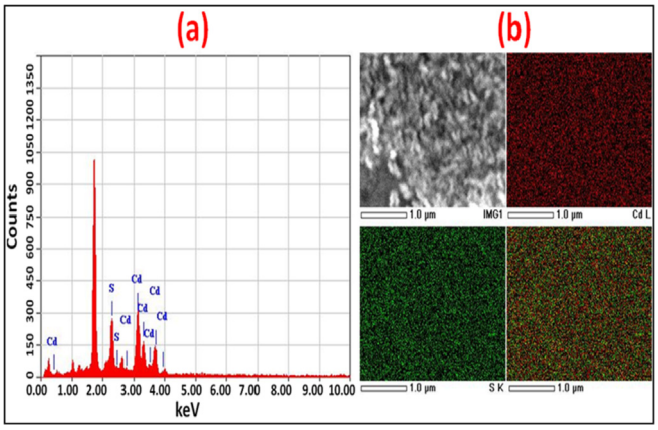

Fig. 2. (a) EDX spectra and (b) SEM mapping image for the deposited CdS thin film.

Table 1
The used atomic percentage and observed atomic percentage of Cadmium and Sulphur elements.

As taken atomic percentage in spray solution (%)		As observed mass percentage in the film by EDX analysis (%)		As observed atomic percentage in the film by EDX analysis (%)		Compositional Ratio (atomic)
Cd	S	Cd	S	Cd	S	S/Cd
50	50	82.01	17.99	56.52	43.48	0.77

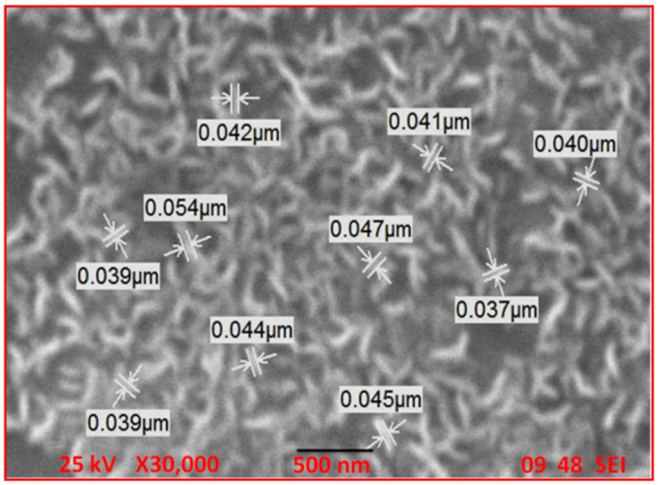

Fig. 3. SEM photograph of the as-prepared CdS thin film.

important parameters as they possess a variety of applications based on morphology and size of grains [37–39]. The average grain size obtained from SEM analysis is 43 nm which slightly differs from the grain size calculated using XRD data. This difference in grain size may be due to cluster formation because of the fusing of two or more grains [32].

3.4. Vibrational analysis

For the investigation of lattice vibrations of as-grown thin film, Raman spectroscopy is an important tool [11,19]. The peak position and width of the Raman spectra can explain the crystallinity quality of the film [19]. Both crystal structures of CdS i.e. cubic and hexagonal have the first (1LO) and second (2LO) order longitudinal optical phonon mode at around 305 cm^{-1} and 600 cm^{-1} respectively [11,35]. Fig. 4 shows the FT-Raman spectra, for as-deposited film, measured in

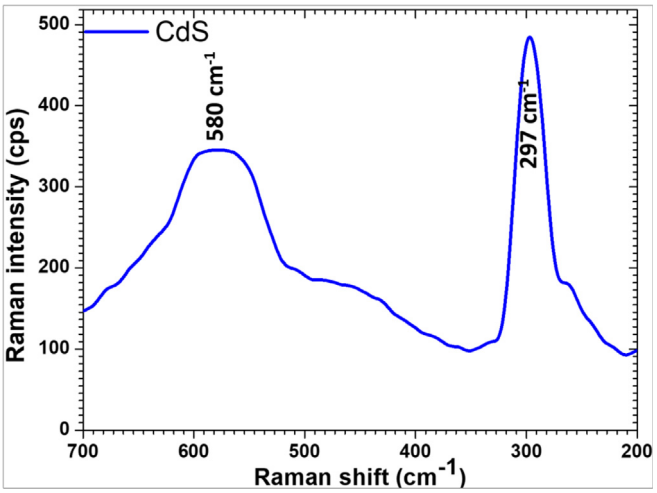

Fig. 4. FT-Raman spectra of CdS thin film recorded at λ_{exc} = 532 nm.

the region of 100–700 cm^{-1} excited at 532 nm wavelength. It can be seen from the figure that, each peak is corresponding to the longitudinal optical phonon mode (LO), 1LO mode is at 297 cm^{-1} which corresponds to scattering by cadmium sulphide longitudinal phonons and its overtone 2LO mode is at 580 cm^{-1}.

The observed Raman shift is comparative to the large-scale CdS, which justify the surface optical phonon mode effect. It can also be concluded from Raman spectra of deposited film that films exhibited good crystallinity. The similar behaviour is observed by other researchers also [19].

3.5. Optical studies

3.5.1. Absorbance, transmittance and reflectance analysis

Among all the II-VI group binary, semiconductors CdS is an extremely light-sensitive material with highly suitable features for optoelectronic applications. Fig. 5(a), (b) & (c) shows the measured absorbance, transmittance and reflectance versus wavelength respectively, for the as-prepared CdS thin film.

The prepared films possess the low absorbance and reflectance with high transmittance which indicates films possess excellent optical transparency which makes them useful in optical window applications. The highest reflectance value was observed at 533 nm wavelength. The prepared film possesses the transmittance of more than 75%. Transmittance at lower wavelength side ($\lambda < 500$ nm) is very less this is because the lower wavelength photons have adequate energy and can excite the electrons to the conduction band. Such type of behaviour of CdS thin films is also reported by other researchers also [16].

3.5.2. Optical band gap study

The band gap of semiconductor nanomaterial is one of the important factors for their applications in optoelectronic devices [19,40]. The band gap of the deposited film was determined using Tauc's equation [40,41] as $\alpha h\nu = A(h\nu - E_g)^s$ where α stands for absorption coefficient, hυ stands for the incident photon energy, E_g stands for energy band gap, A stands for a constant related to the energy of the material and s stands for the empirical constant which takes values s = ½ for direct and s = 2 for indirect allowed transitions [42]. Fig. 6(a) represents the plot of hυ versus $(\alpha h\upsilon)^2$ and Fig. 6(b) represents the plot of hυ vs. $(\alpha h\upsilon)^{1/2}$ respectively. The extrapolation of the linear portion of curves in Fig. 6(a) and 6(b), up to zero absorption coefficients gives the values of the direct and indirect energy band gap.

If the holes and electrons have the same momentum in both conduction and valence band, a photon can be directly emitted by an electron then it is said to be direct band gap and if the photon is not

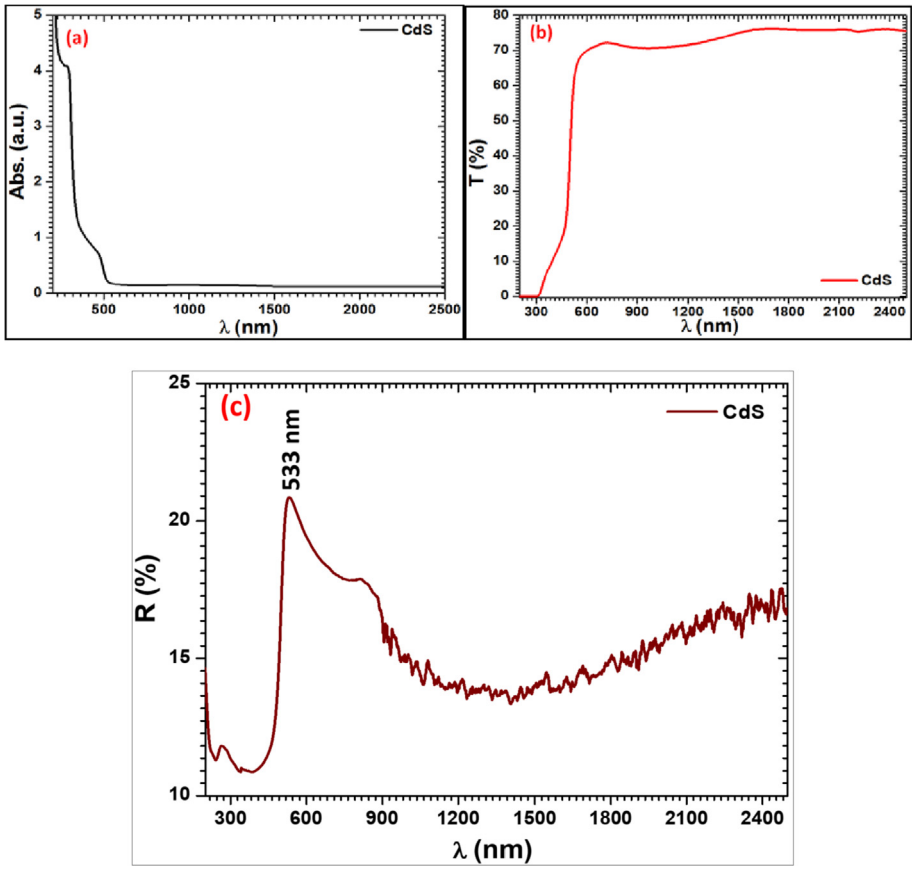

Fig. 5. (a) Absorbance spectra, (b) transmittance spectra and (c) reflectance spectra of as-prepared CdS thin film.

getting emitted directly for that an electron has to go via an intermediate state by transporting momentum to the crystal lattice it is said to be indirect band gap [43]. For the as-deposited film, the calculated value of the direct band gap is 2.43 eV and indirect band gap is 2.23 eV, which are similar to earlier reported valued [25,26,35].

3.5.3. Refractive index and absorption index analysis

Fig. 7 (a) shows the plot of wavelength against absorption index (k) and & Fig. 7(b) shows the plot of wavelength versus refractive index (n).

Absorption index (k) was calculated using the relation [44], $k = \frac{\alpha\lambda}{4\pi}$ and the refractive index (n) was calculated using Fresnel's relation [45], $R = \frac{(n-1)^2+k^2}{(n+1)^2+k^2}$, where R stands for reflectance. Fig. 7(a) shows that the values of absorption index are first decreasing till 500 nm and

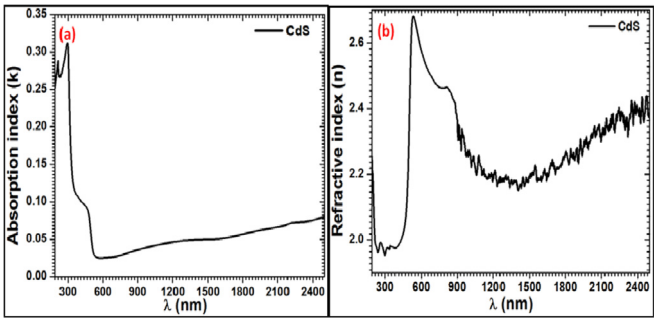

Fig. 7. (a) Absorption index curve and (b) refractive index curve for CdS thin film.

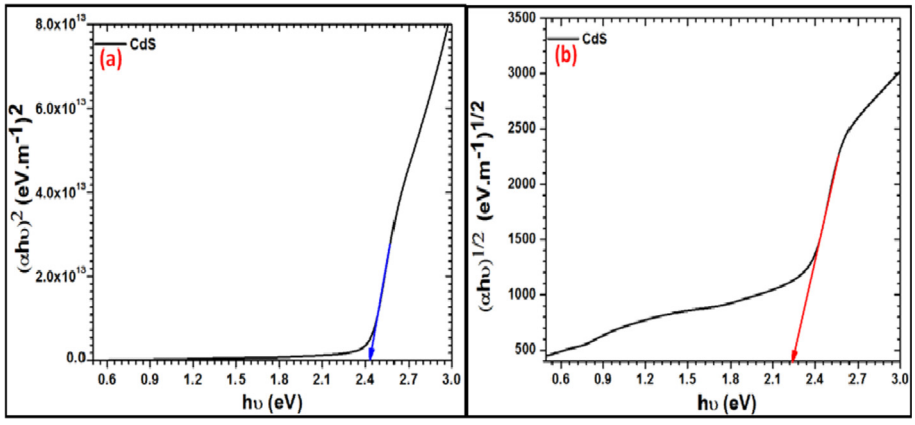

Fig. 6. (a) Direct energy band gap and (b) indirect energy band gap, plots for CdS thin film.

afterwards with an increase in wavelength they are also increasing. The decrease in absorption index with an increase in the wavelength suggests that the fraction of light is departed because of scattering. The speed of light variation, when allowed to fall on a given material, can be analysed using the refractive index. Fig. 7(b) shows that the values of refractive index are increasing with the increase in wavelength, the curve shows a peak in the visible region at 530 nm which arise due to the optical transition in the valence band and conduction band and with further increase in wavelength values of refractive index are decreasing. A similar type of behaviour of k & n is also observed by several researchers [11,19].

3.5.4. Optical dielectric constant study

The optical dielectric constant (ε_1) and optical dielectric loss (ε_2), can explain the sequel of loss of velocity of light and absorption of energy in contrast to the electric field arising from the polarization of particles within the thin film, which is very helpful in studying the electron excitation within thin film [39]. The dielectric constant can elaborate the speed of electromagnetic radiation within the materials and the dielectric loss can explain the absorption of energy of electromagnetic radiation. These parameters were evaluated employing the relations [46]: $\varepsilon_1 = n^2 - k^2$ and $\varepsilon_2 = 2nk$. Fig. 8 (a), (b) and (c) represents the plots of λ versus ε_1, λ versus ε_2 and λ versus loss tangent. Fig. 8(a) shows that the values of dielectric constant are increasing till 600 nm and after that decreasing till 900 nm afterwards becoming almost constant.

Fig. 8(b) shows that values of dielectric loss are higher in low wavelength region which may be the result of the dielectric polarization, it can also be seen that dielectric loss is very less which advocates that the prepared film is defect free which was also confirmed by SEM analysis, this also suggests that the film can be employed for optoelectronic applications. Loss tangent (tanδ) is a measure of signal loss as the signal propagates through the material. A large loss tangent means more dielectric absorption and a lower loss tangent means the large transmission of radiation. From Fig. 8(c) it is clear that the loss tangent has very small values which result in large transmittance as shown in Fig. 5(b).

3.5.5. Optical conductivity and electrical conductivity study

The optical conductivity (σ_{opt}) and electrical conductivity (σ_e) of the prepared sample was calculated using the relations [47]: $\sigma_{opt} = \frac{\alpha nc}{4\pi}$ and $\sigma_e = \frac{2\lambda\sigma_{opt}}{\alpha}$ respectively, where the symbols have their usual meaning. Fig. 9(a) shows the plot of λ versus σ_{opt}, the high and stable values of optical conductivity is the evidence of good photo response and high absorbance at lower wavelengths possess by the prepared film.

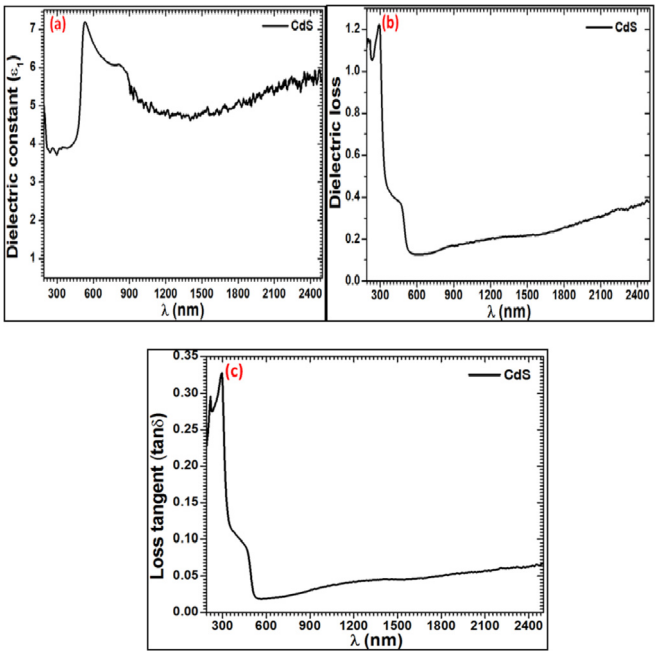

Fig. 8. (a) Dielectric constant curve, (b) dielectric loss curve and (c) loss tangent curve for CdS thin film.

Fig. 9(b) represents the plot of λ versus σ_e, which shows that the electrical conductivity increases with the increasing wavelength. The alike behaviour of the optical conductivity of CdS thin films was reported earlier also [48].

3.6. Electrical conductivity analysis

The electrical conductivity of as-deposited thin film was studied employing D.C. two probe press method at various temperatures successively from 308 to 573 K, under dark. The dc electrical resistivity (ρ) was calculated by means of the relation: $\rho = \frac{RA}{t}$, where R is measured resistance, t is the film thickness and A is the film area under consideration which was taken 2.5 × 1.2 cm^2. The calculated ρ values were fitted into the equation [49]: $\rho = \rho_0 \exp\left(\frac{E_a}{kT}\right)$, where '$E_a$' is activation energy, 'ρ_0' is a constant, 'T' is absolute temperature and 'k' is the Boltzmann constant. The calculated room temperature electrical resistivity for the prepared film is 2.2 × 10^6 Ω-cm, which is in good agreement with values reported earlier [32,49]. Fig. 10 shows the plot of 1000/T versus logρ, which shows the temperature dependence of dark current in the range 300–500 k. It can be seen from the graph that the resistivity of the sample is decreasing with an increase in temperature this authorizes that the prepared films are of semiconductor nature. The value of activation energy E_a is found to be 0.26 eV in the lower-temperature side and 0.82 eV in the higher-temperature side respectively [49,50]. From these activation energy values also the semiconducting nature of the prepared film can be confirmed.

3.7. Thermoelectric power analysis

Thermoelectric power or Seebeck coefficient measurement can reveal the type of conductivity showed by the film, in contrast with the polarity of the thermally produced voltage. For the prepared film, the hot end voltage polarity is positive which indicate that the film possesses n-type conductivity.

4. Conclusions

The thin film of CdS of thickness ~301 nm was deposited facilely on a glass substrate at 300 °C using a modified spray pyrolysis method. XRD analysis discloses that the as-prepared film was of hexagonal phase with polycrystalline nature and grown along (002) orientation. The evaluated average crystallite size from XRD was 15 nm. The presence of cadmium (Cd) and (S) and their composition was confirmed by EDX analysis. SEM analysis reveals that grains are of needle shape which were distributed over the entire film surface and the average grain size from SEM was 43 nm. Raman spectra showed that the 1LO mode is at 297 cm^{-1} and 2LO mode is at 580 cm^{-1}. The optical transparency of grown film is noticed to be high (> 70%), which recommend its use as a window layer in solar cells. The obtained direct optical energy band gap is 2.43 eV. The higher optical conductivity values confirm the high photo response of prepared film. Electrical resistivity at room temperature and activation energy values for the prepared film were found to be 2.2 × 10^6 Ω-cm and 0.26 eV, respectively. The n-type conductivity behaviour of the film is confirmed by thermoelectric power measurement.

Conflicts of interest

Authors declares that there is no conflict of interest in current work.

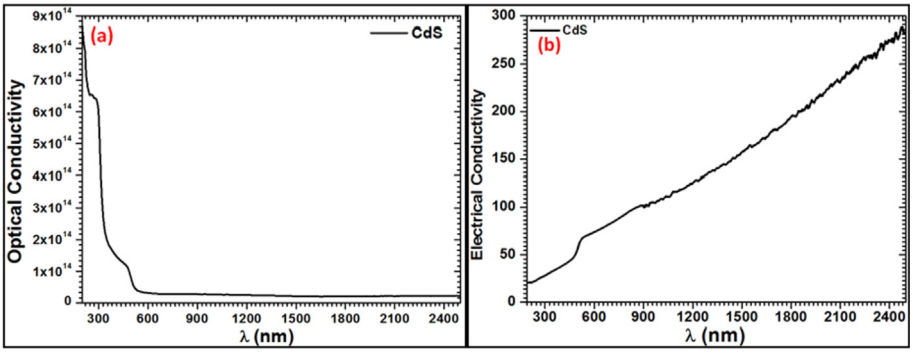

Fig. 9. (a) Optical conductivity and (b) electrical conductivity curve for the prepared CdS film.

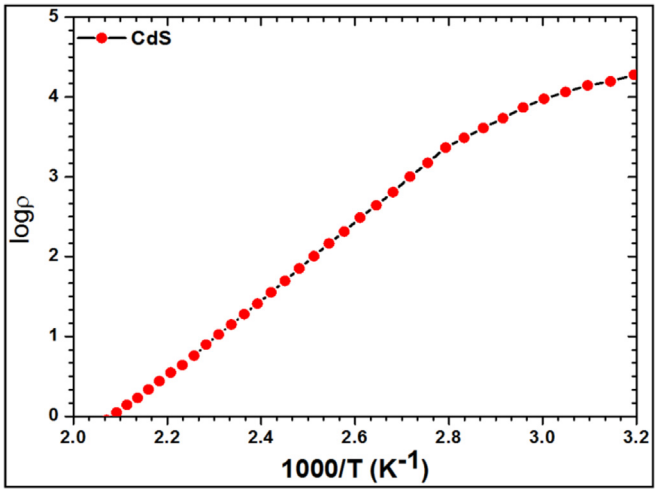

Fig. 10. Plot of the variation of logρ versus 1000/T for the prepared film.

Declaration of interests

The authors declare that they have no known competing financial interests or personal relationships that could have appeared to influence the work reported in this paper.

Acknowledgement

The authors from KKU would like to express their gratitude to deanship of scientific research, King Khalid University, Saudi Arabia for providing the financial support under the project number R.G.P. 2/42/40.

References

[1] A.S. Aybek, M. Kul, E. Turan, M. Zor, E. Gedik, Thermally stimulated currents in CdS film produced by ultrasonic spray pyrolysis method, J. Phys. Condens. Matter 20 (2008) 055216.
[2] D. Zhang, S. Chen, X. Li, Z. Wang, J. Shi, Z. Sun, X. Yin, S. Huang, Cadmium sulfide quantum dots grown by chemical bath deposition for sensitized solar cell applications, Photonics and Optoelectronics Meetings (POEM) 2009: Solar Cells, Solid State Lighting, and Information Display Technologies, International Society for Optics and Photonics, 2009, p. 751804.
[3] J. Meth, S. Zane, G. Nunes Jr., Dual insulated-gate field-effect transistors with cadmium sulfide active layer and a laminated polymer dielectric, Appl. Phys. Lett. 84 (2004) 2922–2924.
[4] R.D. Robinson, B. Sadtler, D.O. Demchenko, C.K. Erdonmez, L.-W. Wang, A.P. Alivisatos, Spontaneous superlattice formation in nanorods through partial cation exchange, Science 317 (2007) 355–358.
[5] R.-M. Ma, L. Dai, G.-G. Qin, High-performance nano-Schottky diodes and nano-MESFETs made on single CdS nanobelts, Nano Lett. 7 (2007) 868–873.
[6] R. Schoolar, Method of Preparation of Lead Sulfide Pn Junction Diodes, Google Patents (1973).
[7] K. Ramanathan, M.A. Contreras, C.L. Perkins, S. Asher, F.S. Hasoon, J. Keane, D. Young, M. Romero, W. Metzger, R. Noufi, Properties of 19.2% efficiency ZnO/CdS/CuInGaSe2 thin-film solar cells, Prog. Photovoltaics Res. Appl. 11 (2003) 225–230.
[8] V. Krishnakumar, J. Han, A. Klein, W. Jaegermann, CdTe thin film solar cells with reduced CdS film thickness, Thin Solid Films 519 (2011) 7138–7141.
[9] G. Sasikala, P. Thilakan, C. Subramanian, Modification in the chemical bath deposition apparatus, growth and characterization of CdS semiconducting thin films for photovoltaic applications, Sol. Energy Mater. Sol. Cells 62 (2000) 275–293.
[10] T.L. Chu, S.S. Chu, Thin film II–VI photovoltaics, Solid State Electron. 38 (1995) 533–549.
[11] Z. Khan, M. Shkir, V. Ganesh, S. AlFaify, I. Yahia, H. Zahran, Linear and nonlinear optics of CBD grown nanocrystalline F doped CdS thin films for optoelectronic applications: an effect of thickness, J. Electron. Mater. 47 (2018) 5386–5395.
[12] H. El Maliki, J. Bernede, S. Marsillac, J. Pinel, X. Castel, J. Pouzet, Study of the influence of annealing on the properties of CBD-CdS thin films, Appl. Surf. Sci. 205 (2003) 65–79.
[13] C. Santiago Tepantlán, A. Pérez González, I. Valeriano Arreola, Structural, optical and electrical properties of CdS thin films obtained by spray pyrolysis, Rev. Mexic. Fisica 54 (2008) 112–117.
[14] F. Lisco, P.M. Kaminski, A. Abbas, K. Bass, J.W. Bowers, G. Claudio, M. Losurdo, J. Walls, The structural properties of CdS deposited by chemical bath deposition and pulsed direct current magnetron sputtering, Thin Solid Films 582 (2015) 323–327.
[15] R. Raffaelle, H. Forsell, T. Potdevin, R. Friedfeld, J. Mantovani, S. Bailey, S. Hubbard, E. Gordon, A. Hepp, Electrodeposited CdS on CIS pn junctions, Sol. Energy Mater. Sol. Cells 57 (1999) 167–178.
[16] P.P. Sahay, R.K. Nath, S. Tewari, Optical properties of thermally evaporated CdS thin films, Cryst. Res. Technol. 42 (2007) 275–280.
[17] B. Sankapal, R. Mane, C. Lokhande, A new chemical method for the preparation of Ag2S thin films, Mater. Chem. Phys. 63 (2000) 226–229.
[18] K. Senthil, D. Mangalaraj, S.K. Narayandass, Structural and optical properties of CdS thin films, Appl. Surf. Sci. 169 (2001) 476–479.
[19] Z.R. Khan, M. Shkir, A.S. Alshammari, V. Ganesh, S. AlFaify, M. Gandouzi, Structural, linear and third order nonlinear optical properties of sol-gel grown Ag-CdS nanocrystalline thin films, J. Electron. Mater. (2019) 1–11.
[20] J. Schaffner, E. Feldmeier, A. Swirschuk, H.-J. Schimper, A. Klein, W. Jaegermann, Influence of substrate temperature, growth rate and TCO substrate on the properties of CSS deposited CdS thin films, Thin Solid Films 519 (2011) 7556–7559.
[21] D. Cameron, W. Duncan, W. Tsang, The structural and electron transport properties of CdS grown by molecular beam epitaxy, Thin Solid Films 58 (1979) 61–66.
[22] D. Patidar, R. Sharma, N. Jain, T. Sharma, N. Saxena, Optical properties of CdS sintered film, Bull. Mater. Sci. 29 (2006) 21–24.
[23] T. Sivaraman, V. Narasimman, V. Nagarethinam, A. Balu, Effect of chlorine doping on the structural, morphological, optical and electrical properties of spray deposited CdS thin films, Prog. Nat. Sci.: Materials International 25 (2015) 392–398.
[24] T. Sivaraman, V. Nagarethinam, A. Balu, CdS thin films fabricated by a simplified spray technique from different substrate temperatures–structural, morphological, optical and electrical analysis, Res. J. Mater. Sci. 2 (2014) 6–15.
[25] S.D. Gunjal, Y.B. Khollam, S.A. Arote, S.R. Jadkar, P.N. Shelke, K.C. Mohite, Structural, optical and electrical properties of spray pyrolysis deposited CdS films, Macromol. Symp. 347 (2015) 9–15.
[26] A. Ashour, Physical properties of spray pyrolysed CdS thin films, Turk. J. Phys. 27 (2004) 551–558.
[27] R. Singh, S. Bhushan, Structural and optical properties of chemically deposited Cd (S-Se): CdCl 2, Sm films, Bull. Mater. Sci. 32 (2009) 125–133.
[28] V. Senthilkumar, S. Venkatachalam, C. Viswanathan, S. Gopal, S.K. Narayandass, D. Mangalaraj, K. Wilson, K. Vijayakumar, Influence of substrate temperature on the properties of vacuum evaporated InSb films, Crystal Research and Technology, Journal of Experimental and Industrial Crystallography 40 (2005) 573–578.
[29] M. Shkir, I.S. Yahia, V. Ganesh, Y. Bitla, I.M. Ashraf, A. Kaushik, S. AlFaify, A facile synthesis of Au-nanoparticles decorated PbI2 single crystalline nanosheets for optoelectronic device applications, Sci. Rep. 8 (2018) 13806.
[30] M. Shakir, S. Kushwaha, K. Maurya, G. Bhagavannarayana, M. Wahab, Characterization of ZnSe nanoparticles synthesized by microwave heating process, Solid State Commun. 149 (2009) 2047–2049.
[31] K. Khot, S. Mali, N. Pawar, R. Mane, V. Kondalkar, V. Ghanwat, P. Patil, C.K. Hong, J.H. Kim, J. Heo, Novel synthesis of interconnected nanocubic PbS thin films by facile aqueous chemical route, J. Mater. Sci. Mater. Electron. 25 (2014) 3762–3770.

[32] A. Yadav, M. Barote, E. Masumdar, Studies on nanocrystalline cadmium sulphide (CdS) thin films deposited by spray pyrolysis, Solid State Sci. 12 (2010) 1173–1177.
[33] H. Khallaf, I.O. Oladeji, G. Chai, L. Chow, Characterization of CdS thin films grown by chemical bath deposition using four different cadmium sources, Thin Solid Films 516 (2008) 7306–7312.
[34] J. Lee, Raman scattering and photoluminescence analysis of B-doped CdS thin films, Thin Solid Films 451 (2004) 170–174.
[35] H. Algarni, A.E. Al-Salami, A.A. Alshahrani, T.F. Alhuwaymel, A. Al-Mogeeth, A noticeable effect of thickness on third order nonlinear properties of CBD grown CdS thin films investigated by Z-scan measurements, Optik 181 (2019) 146–155.
[36] S.J. Ikhmayies, R.N. Ahmad-Bitar, The influence of the substrate temperature on the photovoltaic properties of spray-deposited CdS:In thin films, Appl. Surf. Sci. 256 (2010) 3541–3545.
[37] D. Sengupta, P. Das, B. Mondal, K. Mukherjee, Effects of doping, morphology and film-thickness of photo-anode materials for dye sensitized solar cell application – a review, Renew. Sustain. Energy Rev. 60 (2016) 356–376.
[38] M. Shkir, M.T. Khan, S. AlFaify, Novel Nd-Doping Effect on Structural, Morphological, Optical, and Electrical Properties of Facilely Fabricated PbI2 Thin Films Applicable to Optoelectronic Devices, Applied Nanoscience, 2019.
[39] J.L. Castro-Mayorga, M.J. Fabra, A.M. Pourrahimi, R.T. Olsson, J.M. Lagaron, The impact of zinc oxide particle morphology as an antimicrobial and when incorporated in poly(3-hydroxybutyrate-co-3-hydroxyvalerate) films for food packaging and food contact surfaces applications, Food Bioprod. Process. 101 (2017) 32–44.
[40] M. Shkir, H. Abbas, Z.R. Khan, Effect of thickness on the structural, optical and electrical properties of thermally evaporated PbI < sub > 2 thin films, J. Phys. Chem. Solids 73 (2012) 1309–1313.
[41] M. Shkir, A. Khan, A.M. El-Toni, A. Aldalbahi, I.S. Yahia, S. AlFaify, Structural, morphological, opto-nonlinear-limiting studies on Dy:PbI2/FTO thin films derived facilely by spin coating technique for optoelectronic technology, J. Phys. Chem. Solids 130 (2019) 189–196.
[42] M. Shkir, Structural, optical and electrical properties of znse semiconductor nanoparticles, Chalcogenide Lett. 8 (2011) 435–440.
[43] M. Shkir, V. Ganesh, S. AlFaify, I. Yahia, H. Zahran, Tailoring the linear and nonlinear optical properties of NiO thin films through Cr 3+ doping, J. Mater. Sci. Mater. Electron. 29 (2018) 6446–6457.
[44] M. Shkir, V. Ganesh, S. AlFaify, I.S. Yahia, Structural, linear and third order nonlinear optical properties of drop casting deposited high quality nanocrystalline phenol red thin films, J. Mater. Sci. Mater. Electron. 28 (2017) 10573–10581.
[45] E. Tikhonov, V. Ivashkin, A. Ljamec, Reflection refractometry for nearly normal incidence and at the Brewster angle, J. Appl. Spectrosc. 79 (2012) 148–156.
[46] M.-S. Kim, K.-G. Yim, J.-S. Son, J.-Y. Leem, Effects of Al concentration on structural and optical properties of Al-doped ZnO thin films, Bull. Korean Chem. Soc. 33 (2012) 1235–1241.
[47] T. Girisun, S. Dhanuskodi, Linear and nonlinear optical properties of tris thiourea zinc sulphate single crystals, Cryst. Res. Technol. 44 (2009) 1297–1302.
[48] A.J. Khimani, S.H. Chaki, T.J. Malek, J.P. Tailor, S.M. Chauhan, M. Deshpande, Cadmium sulphide (CdS) thin films deposited by chemical bath deposition (CBD) and dip coating techniques—a comparative study, Mater. Res. Express 5 (2018) 036406.
[49] M.A. Barote, A.A. Yadav, E.U. Masumdar, Synthesis, characterization and photoelectrochemical properties of n-CdS thin films, Phys. B Condens. Matter 406 (2011) 1865–1871.
[50] S. Suresh, Studies on the dielectric properties of CdS nanoparticles, Appl. Nanosci. 4 (2014) 325–329.